SUPPORTING INFORMATION

Efficient Recognition of an Unpaired Lesion by a DNA Repair Glycosylase

Derek M. Lyons and Patrick J. O'Brien*

Department of Biological Chemistry, University of Michigan, Ann Arbor, Michigan 48109-0606

† This work was supported by a grant from the NIH to P.O. (CA122254). D.L. was supported in part by an NIH training grant at the Chemistry/Biology Interface.

* To whom correspondence should be addressed. Phone: 734-647-5821. E-mail: pjobrien@umich.edu.

Materials and methods and supporting results and discussion are provided here. Figure S1 shows the sequence of the oligonucleotide substrates. A representative gel and accompanying time course are shown for the single turnover glycosylase assay (Figure S2). Additional representative exponential fits are shown for reactions with rate constants that varied by 4 orders of magnitude (Figure S3). The concentration dependence of the single turnover reaction for mismatch and bulge substrates from Figure 2 in the text have been replotted with more appropriate scales (Figure S4). The AAG concentration dependence for two single-stranded inosine-containing oligonucleotides is displayed in Figure S5. The similar behavior for two different oligonucleotides, one of which is flanked by poly-thymidine stretches, suggests that the observed reaction took place on a single-stranded oligonucleotide. Several previous studies have examined the glycosylase activity of AAG towards single-strand and mismatched oligonucleotides substrates. These supporting references are provided and our results are discussed in the context of the other relevant studies.

MATERIALS AND METHODS

Expression and Purification of Recombinant AAG. The catalytic fragment of AAG lacking the first 79 amino acids (Δ80) was expressed in *E. coli* and purified as previously described.[1] The truncated protein has a slightly decreased ability to translocate along DNA, relative to the full-length enzyme, but both proteins have identical glycosylase activity towards inosine and 1,N^6-ethenoadenosine lesions.[2,3] The concentration of active enzyme was determined by burst analysis as described below and the concentration of active enzyme was used throughout.

Oligonucleotide Substrates. The sequences and annealed structures of the DNA oligonucleotides used in this study are given in Figure S1. The lesion-containing 25mer oligonucleotides have a centrally located inosine lesion and include a 5'-fluorescein (6-fam) label. Complementary strands are unlabeled. The DNA oligonucleotides were synthesized by commercial sources using standard phosphoramidite chemistry, and were purified by denaturing polyacrylamide gel electrophoresis on a 20% polyacrylamide gel (6.6 M urea and Tris-borate buffer; 89 mM tris, 89 mM borate, 2 mM EDTA). Full-

length oligonucleotides were excised from the gel, crushed, and soaked overnight in 500 mM NaCl and 1mM EDTA. Desalting was accomplished by reverse phase chromatography (C18 Sep-pak, Waters). Concentrations of single-stranded oligonucleotides were determined by absorbance at 260 nm using the calculated extinction coefficients. For glycosylase assays, oligonucleotides were annealed with a 1.5-fold excess of complementary strand, heated to 90˚C and subsequently cooled to 4˚C over ~15 min.

General Glycosylase Assay. Samples were quenched with two volumes of 0.3 M NaOH to obtain a final concentration of 0.2 M. Abasic sites were quantitatively converted to DNA breaks by heating at 70˚C for 15 min, followed by the addition of 3.3 volumes of formamide/EDTA loading buffer that contained 0.05% w/v of both bromophenol blue and xylene cyanol FF as tracking dyes. DNA substrate (25mer) and cleaved product (12mer) oligonucleotides were separated on a 20% denaturing polyacrylamide gel containing 6.6 M urea. A typhoon trio imager was used to scan the gels with a 488 nm excitation and 520 nm long pass filter to detect the fluorescein labeled oligonucleotides. The substrate and product bands were quantified with Image Quant TL (GE Healthcare) and the fraction product formed at each time point was calculated by [F = P/(P+S)], in which F is the fraction converted to product, P is the fluorescence of the product, and S is the fluorescence of the intact substrate. Control reactions in which enzyme was omitted revealed that inosine-containing oligonucleotides were stable to this procedure and no product was detected in the absence of glycosylase.

Burst Analysis to Determine Active AAG Concentration. The active concentration of recombinant AAG was determined by burst analysis as previously described.[2] With a fixed concentration of 1μM of I•T 25mer substrate, which is far above the $K_{d,}$ the concentration of AAG was varied to obtain a burst of 5-20%. The fraction product was determined by polyacrylamide gel electrophoresis, as described above, and converted into concentration of product by multiplying by the concentration of initial substrate. The production of product followed an initial burst, followed by a slow multiple turnover rate. The reaction progress curve was fit by equation S2 using Kaleidagraph, in which P is

product, A is the burst amplitude, k_{obs} is the burst rate constant, and V_{obs} is the steady state velocity. The burst amplitude gives the concentration of active enzyme.

$$[P] = A[1-\exp(-k_{obs}t)] + V_{obs}t \quad \text{(S1)}$$

Single Turnover Assay for Glycosylase Activity. Single turnover glycosylase assays were performed with AAG in excess over the 0.1 μM DNA substrate. The standard conditions were 23 ^{o}C, 50 mM NaMES (pH 6.0), 1 mM EDTA, 1 mM DTT, 10% (v/v) glycerol, 0.1 mg/mL BSA, and the ionic strength was adjusted to 200 mM with NaCl. Typical reaction volumes were 20 μL, with 3 μL aliquots being removed at the desired time and quenched in NaOH and analyzed as described above. To determine the rate constant, time points were taken over the entire reaction progress curve and the fraction of product was plotted as a function of reaction time. Data analysis was performed using Kaleidagraph. In all cases, the reaction progress curves followed a single exponential and were fit by Equation S2, in which A is the fraction of substrate converted to product at completion ($A \geq 0.94$), k_{obs} is the observed single turnover rate constant, and t is the reaction time. Fits were excellent in all cases ($R^2 \geq 0.97$).

$$F = A[1-\exp(-k_{obs}t)] \quad \text{(S2)}$$

For extremely fast reactions, with half-lives of less than 20 s, some modifications to this protocol were made. Equal volumes (3 μL) of enzyme and substrate were mixed by hand, with the reaction occurring in the pipet tip, and subsequently quenched in a tube containing 6 μL of 0.3 M NaOH. The concentrations indicated throughout are for the final reaction mixture after mixing substrate and product. With the assistance of a metronome, time points could be accurately and reproducibly quenched at times as fast as 4 s.

For each substrate, we determined the concentration dependence by varying the concentration of AAG under single turnover conditions ([AAG] ≥ [DNA]). The rate constants for 4-8 independent reactions were averaged and the standard deviation was calculated in Excel. Plots of the observed rate constant as a function of the concentration

of AAG were fit by a hyperbolic equation analogous to the Michaelis-Menten Equation (Eq. S3), in which the maximal observed rate constant (k_{max}) corresponds to the rate of the reaction at a saturating concentration of enzyme and the $K_{1/2}$ value indicates the concentration at which half of the substrate is bound. The ratio of $k_{max}/K_{1/2}$ is analogous to the steady state rate constant k_{cat}/K_M, which is commonly referred to as catalytic efficiency. Comparison of k_{cat}/K_M values for different substrates takes into account differences in both binding and catalysis.

$$k_{obs} = k_{max}[AAG]/(K_{1/2} + [AAG]) \quad \text{(S3)}$$

Free Energy Calculations. A linear free energy relationship correlating the catalytic efficiency of different inosine mismatches with the thermodynamic duplex stability demonstrates an inverse relationship between duplex stability and catalytic efficiency. The ΔΔG value for the relative catalytic efficiencies were calculated according to the equation, $\Delta\Delta G = -RT \ln(k_{cat}/K_M^{rel})$, in which k_{cat}/K_M^{rel} is the ratio of the k_{cat}/K_M value for the mismatch divided by that of the fastest substrate, the single nucleotide bulge (Table S2). The ΔΔG values for duplex stability were calculated from a comprehensive study of the nearest neighbor effects on duplex stability of inosine-containing DNA oligonucleotides, as described in Table S1.[4]

SUPPORTING RESULTS AND DISCUSSION

Evaluation of data quality. Representative time courses are shown for the single turnover glycosylase activity of AAG on the slowest substrates, single-stranded DNA, and the fastest substrate, the single nucleotide bulge DNA (Figure S2). These plots demonstrate that fast and slow reactions all followed the expected single exponential. This indicates that AAG is stable under these assay conditions, and that fast time points could be reliably taken by hand.

Minimal kinetic scheme to interpret single turnover experiments. Multiple turnover glycosylase activity of AAG is limited by product release under many conditions. Therefore we have used single turnover conditions to monitor the steps up to and including the first irreversible step, hydrolysis of the N-glycosidic bond (Scheme S1). Under these conditions, the observed maximal rate constant (k_{max}) could be limited by either the nucleotide flipping step or the N-glycosidic bond hydrolysis step. The $K_{1/2}$ value is likely to reflect the K_d for substrate dissociation, since pulse-chase experiments show that dissociation is much faster than the forward rate constant for the reaction (O'Brien, data not shown). However, dissociation could involve one or two steps, depending on whether the flipping equilibrium is favorable or unfavorable. Regardless of whether the equilibrium for nucleotide flipping is favorable or not, the ratio $k_{max}/K_{1/2}$ is analogous to k_{cat}/K_M and this second order rate constant monitors all of the steps of the reaction going from free substrate in solution to a transition state on the enzyme that has a flipped-out lesion nucleotide. We refer to this second order rate constant as k_{cat}/K_M for simplicity.

Activity of AAG towards mismatches and a single nucleotide bulge. The single turnover rate constants for the substrates mentioned in the main text and an additional single-stranded substrate are summarized in Table S2. The best fit of the concentration dependence is reported and the error was estimated by fitting the concentration dependence of all of the independently determined rate constants (from ~50 individual single turnover reactions) with a hyperbolic equation (Eq. S2) using Kaleidagraph.

The full single turnover characterization of inosine-mismatches has not been previously reported for any sequence context, but several previous studies have tested whether the opposing base has an effect on the maximal single turnover rate constant. These are summarized in Table S3. The maximal rate constants that we report with a fluorescence-based glycosylase assay are within 2-fold of the values reported previously using a ^{32}P-based assay.[5] This suggests that the change in reaction conditions and in labeling method does not have a substantial effect on AAG catalysis. The differences between I•T and I•C range from 2–5 fold for different sequence contexts and different reaction conditions. Other studies have used a fixed concentration of AAG and DNA to report initial rates for glycosylase activity towards inosine mismatches.[6-8] These studies found much larger effects, with the I•T mismatch being acted upon with 10 to 50-fold faster a rate than the I•C mismatch. The 24-fold greater catalytic efficiency towards I•T than I•C that we have measured for k_{cat}/K_M suggests that the previously published results also compared k_{cat}/K_M. Since the competition between substrates is determined by their relative k_{cat}/K_M values, this indicates that AAG has a strong preference towards an I•T mismatch in many different sequence contexts,.

Since we have analyzed the full concentration dependence, these data allow us to confirm that most of the difference in k_{cat}/K_M is attributed to a difference in binding affinity, with relatively small differences in reaction rate once the substrate is bound (Table S2). The origin of this large difference in ground state binding is currently unclear. One possible explanation is that the ground state complex is stably flipped (K_{flip} >>1; as has recently been observed for the 1,N^6-ethenoadenosine lesion (Wolfe & O'Brien, submitted). In this case, the more stable base pairs will require additional binding energy to reconfigure the substrate and flip out the inosine lesion and this will be reflected in a weaker affinity. However, we cannot rule out the possibility that the opposing base is directly contacted in an initial recognition complex that differs from the specific lesion recognition complex that has been observed crystallographically and that shows no specific contacts to the opposing base.[9,10] Stopped-flow binding of 1,N^6-ethenoadenosine to AAG provides evidence that such an intermediate exists for this substrate (Wolfe & O'Brien, submitted). Future studies looking directly at the rate and equilibrium constant

for flipping of inosine from different sequence contexts will be required to address this issue.

A previous study concluded that an opposing base is required for AAG glycosylase activity because a lesion that was placed opposite a reduced abasic site (tetrahydrofuran) was not a substrate for AAG.[11] However, it is not possible to rule out the possibility that AAG binds to the reduced abasic site directly since AAG binds with high affinity to this product mimic when it is across from a normal pyrimidine.[11] The finding that a single nucleotide bulge is an excellent substrate for AAG demonstrates unequivocally that an opposing base is not required. Therefore, the decrease in glycosylase activity across from an abasic site is due either to inhibition (binding directly to the abasic site) or to an alternative conformation that is less efficiently recognized by AAG.

Activity of AAG towards single-stranded inosine-containing DNA. It has previously been reported that AAG has no detectable glycosylase towards inosine in single-stranded DNA.[12] This is in contrast to oxanine and 1,N^6-ethenoA for which double stranded DNA is only modestly preferred by AAG.[13] A recent report concluded that AAG also has robust activity towards inosine in a single-strand[14], but these reactions did not appear to go to completion and it was noted that the sequence of the oligonucleotide that was used was self-complementary in the region of the inosine lesion, which raises the possibility that the activity observed was not towards a single-stranded lesion. We find that the single-stranded oligonucleotide that we have characterized is an extremely poor substrate for AAG, with maximal saturating (k_{max}) and sub-saturating (k_{cat}/K_M) rate constants that are more than 2000-fold slower than those that were measured for the I•T mismatch (Table S2). Although the sequence that we initially used is not predicted to form stable secondary structure, we were concerned that a high concentration of AAG might stabilize an otherwise unstable structure that would allow faster rate of excision. In this case, these large effects might overestimate the activity of AAG on single-stranded inosine. Therefore, we designed a sequence that was all pyrimidines except for the central inosine lesion, by replacing the flanking nucleotides with thymidines. The single turnover excision data for this alternative sequence (ssT) is summarized in Figure S5 and Table

S2. The less diverse sequence bound 2.5-fold weaker and had a maximal rate that was 2-fold slower than the heterogenous sequence. This corresponds to a 5-fold decrease in the catalytic efficiency for the all-pyrimidine sequence (Table S2). It is not clear what the origin of this sequence preference is, but it could reflect some effect of secondary structure in the heterogenous sequence or could reflect sequence-specific binding of AAG to positions more than 2 nucleotides upstream or downstream of the lesion. These results indicate that an I lesion in single-stranded DNA is a very poor substrate for AAG. Presumably the large entropic cost of positioning the inosine lesion and surrounding DNA into an active site designed for a duplex substrate accounts for the large decrease in catalytic efficiency towards a single-stranded substrate.

A linear free energy relationship for the inosine DNA glycosylase activity of AAG. The barrier to nucleotide flipping can be evaluated by comparing the activity of the enzyme towards a lesion that is present in different base pairing contexts. The rate constant k_{cat}/K_M monitors the differences in energy between the ground state duplex in solution and the transition state bound to the enzyme with the lesion flipped out. Since the bond being broken is identical in each case, the transition state is the same for each mismatch. Therefore, differences in reaction rate between different mismatches will be dominated by specific differences between the different base pairs. We have used the available data for the contributions of inosine mismatches to the equilibrium constant for duplex stability. Duplex stability is expected to be sensitive to how well a given mismatch is accommodated in the duplex and therefore serves as a useful surrogate for the base pairing stability of a given mismatch. The relative duplex stability for the sequence context that we used were calculated as described in the Materials and Methods and outlined in Table S1. The relative k_{cat}/K_M values for AAG-catalyzed glycosylase activity were also converted into changes in free energy ($\Delta\Delta G$) and plotted in the text (Figure 3). Since only the natural I mismatches were used this is a very limited data set. It will be necessary to look at a larger set of natural and unnatural base pairs in order to obtain sufficient confidence in the exact slope. Nevertheless, the observed slope is sufficiently steep that we believe that the general trend is informative.

The best linear fit gives a slope of -0.96 (R^2=0.67). This strong negative correlation indicates that the differences in duplex stability for the different mismatches are fully realized in going from the ground state to an extrahelical AAG-bound transition state. The observation of a linear relationship between activity and duplex stability is consistent with the absence of specific contacts between AAG and the opposing base.[9,10] However, this conclusion is tenuous because there is a large deviation between the two least stable mismatches (I•T and I•G). If I•G deviates due to a negative effect, then the slope would be considerably steeper. If I•T deviates due to a positive effect, then the slope is less steep (slope = -0.6; R^2 = 0.97). Since the biological function of AAG is to recognize and repair I•T mismatches, the natural context for deamination of an adenosine in DNA, it is plausible that additional factors beyond duplex destabilization lead to more efficient recognition by AAG. Previously it has been suggested that the unique wobble base pair geometry that is formed by an I•T pair could be responsible for the more efficient recognition by AAG.[11]

A comprehensive analysis of the enthalpic and entropic components of nucleotide flipping by uracil DNA glycosylase have revealed a variety of factors involved in influencing the barrier to binding and flipping by this enzyme [15-18]. These barriers include stable hydrogen bonds and duplex rigidity, both of which are reduced by mismatched base pairs. In the future it will be interesting to learn to what extent evolutionarily distinct nucleotide flipping enzymes share mechanistic similarities.

Scheme S1. Minimal kinetic scheme for single turnover glycosylase activity of AAG

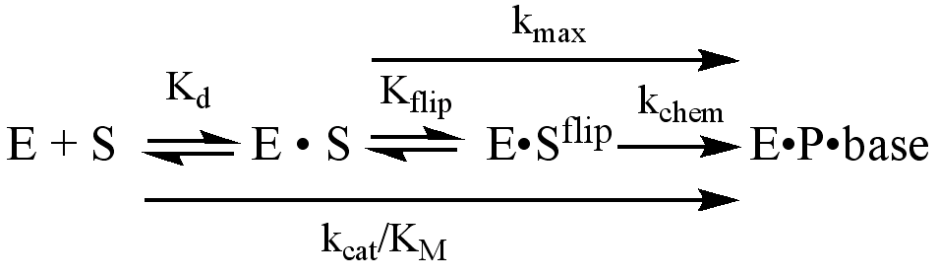

Table S1. Calculation of relative duplex stabilities for the inosine mismatches

	–TIC– –AXG–			
	X=C	X=A	X=T	X=G
ΔG TI/AX	-0.46 ± 0.06	0.09 ± 0.06	0.36 ± 0.06	0.76 ± 0.06
ΔG IC/XG	-1.07 ± 0.08	-1.33 ± 0.08	-0.54 ± 0.08	-0.74 ± 0.08
ΔG TIC/AXG	-1.53 ± 0.14	-1.24 ± 0.14	-0.18 ± 0.14	0.02 ± 0.14
ΔΔG	(0) ± 0.28	0.29 ± 0.28	1.35 ± 0.28	1.55 ± 0.28

Duplex stabilities were calculated using nearest neighbor rules from a systematic study of duplex stability for inosine mismatches in different sequence contexts.[4] All values are expressed in units of kcal/mol. The difference in free energy (ΔΔG is calculated by subtracting the value of ΔG for the most stable pair (I•C) from the ΔG for the indicated pair and therefore ΔΔG for I•C is defined as zero.

Table S2. Kinetic parameters for single turnover inosine DNA glycosylase activity of AAG[a]

Opposing Base	$K_{1/2}$ (μM)	k_{max} (min^{-1})	k_{cat} / K_M [b] ($M^{-1}s^{-1}$)	Relative k_{cat}/K_M [c]
None (bulge)	0.080 ± 0.008[d]	5.4 ± 0.1	$1.1 \pm 0.1 \times 10^6$	3.2
T	0.30 ± 0.02	6.3 ± 0.1	$3.5 \pm 0.2 \times 10^5$	(1)
G	0.41 ± 0.05	1.5 ± 0.1	$6.2 \pm 0.8 \times 10^4$	0.18
C	3.8 ± 0.6	3.3 ± 0.2	$1.4 \pm 0.2 \times 10^4$	0.041
A	2.3 ± 0.5	2.0 ± 0.1	$1.4 \pm 0.3 \times 10^4$	0.041
Single-strand ss[e]	0.34 ± 0.06[d]	0.0035 ± 0.0002	$1.7 \pm 0.1 \times 10^2$	0.00048
Single-strand ssT[e]	0.86 ± 0.09	0.0017 ± 0.0001	$3.2 \pm 0.3 \times 10^1$	0.000095

A simplified form of this table is shown in the text (Table 1). [a]Data were collected at 23 °C in 50 mM NaMES, pH 6.1, 1 mM EDTA, 1 mM DTT, 0.1 mg/mL BSA and with an ionic strength of 200 mM (adjusted with NaCl). [b]k_{cat}/K_M is calculated from the ratio of $k_{max}/K_{1/2}$, since this process monitors the same steps as k_{cat}/K_M in steady state kinetics. [c]The relative k_{cat}/K_M value was obtained by dividing the k_{cat}/K_M for a given substrate by the k_{cat}/K_M value for the I•T mismatch. [d]These values of $K_{1/2}$ are similar to the concentration of substrate (0.1 μM), so they should be considered upper limits to the true $K_{1/2}$ value. If the $K_{1/2}$ value is significantly lower, then the k_{cat}/K_M value would be higher. [e]The two different single-stranded sequences that were tested are shown in Figure S1. The errors for the k_{max} and $K_{1/2}$ values were estimated from curve fitting using nonlinear least squares regression to fit a hyperbolic concentration dependence (Equation S3) to all of the individual values of k_{obs} determined for a given substrate (Kaleidagraph), and this error was propagated to determine the error in k_{cat}/K_M.

Table S3. Comparison of k_{max} values for the glycosylase activity of AAG towards inosine in different mismatches

		Normalized k_{max}			
Sequence	Reference	I•T	I•G	I•C	I•A
–TIC–	This study	(1)	0.24	0.52	0.32
–TIC–	5	(1)	0.14	0.40	0.18
–GIG–	8	(1)	0.31	0.31	0.11
–TIG–	11	(1)	ND	0.19	ND

The saturating single turnover rate constant, k_{max}, was normalized by dividing the value for a given mismatch by that of the most active mismatch context I•T. ND, not determined.

Figure S1. Sequence of oligonucleotides that were used in this study. The inosine-containing strands had a 5'-fluorescein attached by a 6-aminohexyl linker (fam).

```
I•T       5'fam-CGATAGCATCCTICCTTCTCTCCAT
             3'-GCTATCGTAGGATGGAAGAGAGGTA

I•C       5'fam-CGATAGCATCCTICCTTCTCTCCAT
             3'-GCTATCGTAGGACGGAAGAGAGGTA

I•A       5'fam-CGATAGCATCCTICCTTCTCTCCAT
             3'-GCTATCGTAGGAAGGAAGAGAGGTA

I•G       5'fam-CGATAGCATCCTICCTTCTCTCCAT
             3'-GCTATCGTAGGAGGGAAGAGAGGTA

                              I
I bulge   5'fam-CGATAGCATCCTCCTTCTCTCCAT
             3'-GCTATCGTAGGAGGAAGAGAGGTA

I (ss)    5'fam-CGATAGCATCCTICCTTCTCTCCAT

I (ssT)   5'fam-TTTTTTTTTTCTICCTTTTTTTTT
```

Figure S2. Representative single turnover glycosylase assay. (A) The fluorescence scan of a 20% polyacrylamide gel shows a reaction time course with 1μM AAG and 0.1μM I bulged substrate. The 25mer substrate is converted into a 12mer product after AAG-catalyzed N-glycosidic bond cleavage and alkaline cleavage of the abasic site. A control reaction in which AAG was omitted demonstrates that the inosine-containing substrate is stable to the glycosylase assay and provides the background signal expected at the initiation of the reaction. (B) The quantified data is fit to a single exponential curve (Eq. S2) and gives a k_{obs} value of 5.5 min^{-1} with an R^2 value of 0.99. Several independent experiments were performed for each concentration of AAG and the average and standard deviation are reported in Figure S3.

(A)

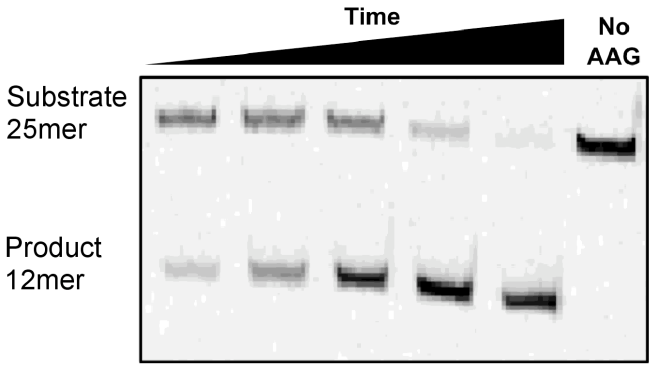

(B)

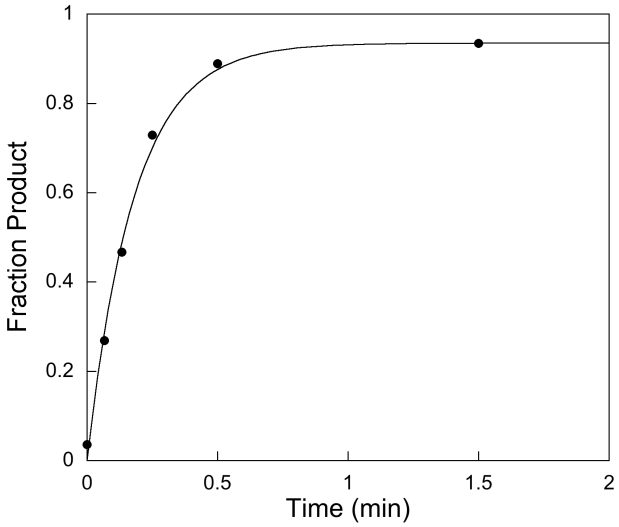

Figure S3. Representative data for single turnover glycosylase activity with the slowest and fastest substrates. (A) For the thymidine-rich single-stranded substrate time points were taken over >3 days and the triplicate reactions are shown with saturating (15 μM) and sub-saturating (0.2 μM) AAG. (B) For the single nucleotide bulge substrate, time points were taken from 4-150 s. Duplicate reactions at saturating (3 μM) and subsaturating (0.1 μM) AAG are shown. For all substrates and all concentrations of AAG the reaction progress curves followed single exponentials and went to a similar endpoint of ≥95% cleaved.

(A)

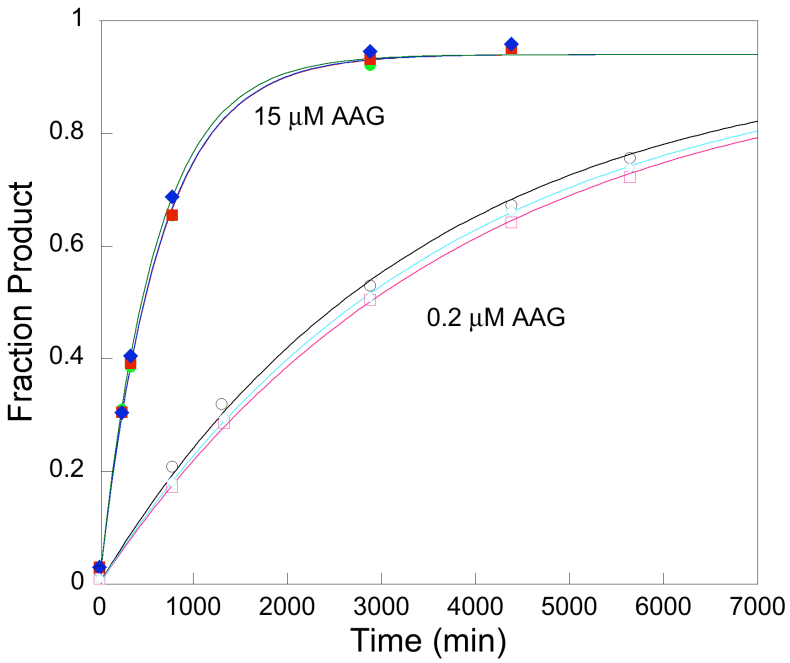

(B)

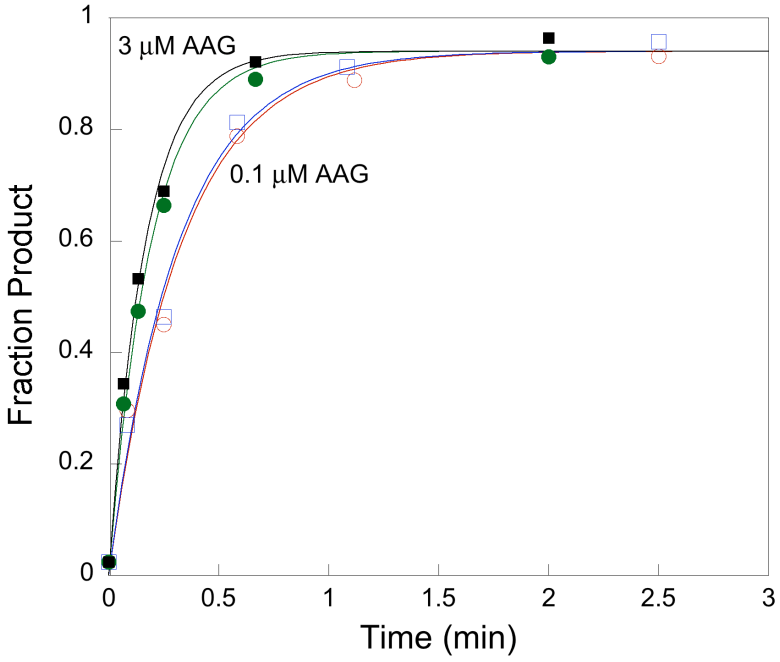

Figure S4. Concentration dependence for the inosine DNA glycosylase activity of AAG replotted from Figure 2 in the text. The axes were adjusted to facilitate comparison of individual substrates. (A) The I·T mismatch (●) and the I bulge (■) show very similar single turnover kinetics. (B) AAG shows decreased glycosylase activity towards I·C (◆), I·A (●), and I·G mismatches (■) with decreases in k_{max} and increases in $K_{1/2}$ (See Table S2 for the kinetic values and error estimates for the different substrates).

(A)

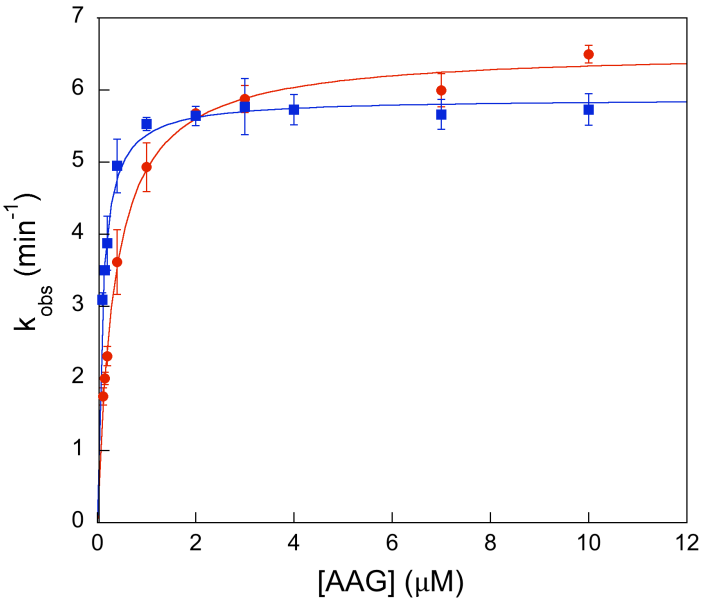

(B)

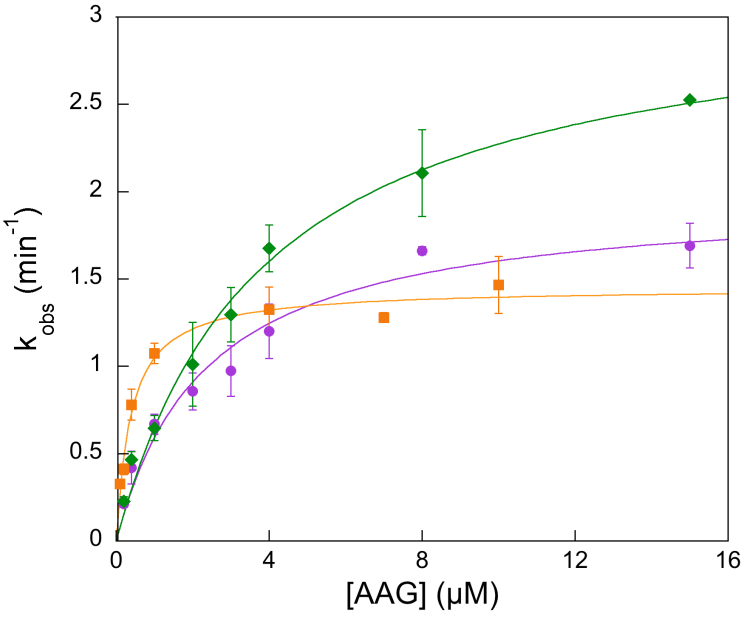

Figure S5. Single turnover inosine DNA glycosylase activity of AAG for single-stranded substrates. The data for the heterogenous sequence (ss, ●) and the T-rich sequence (ssT, ■) are directly compared. See Figure 1 for the complete oligonucleotide sequences. Each point indicates the average of 3-6 independent determinations and the error bars indicate one standard deviation from the mean. In several cases the error bars are smaller than the symbols that were used. The single turnover rate constants are given in Table S2.

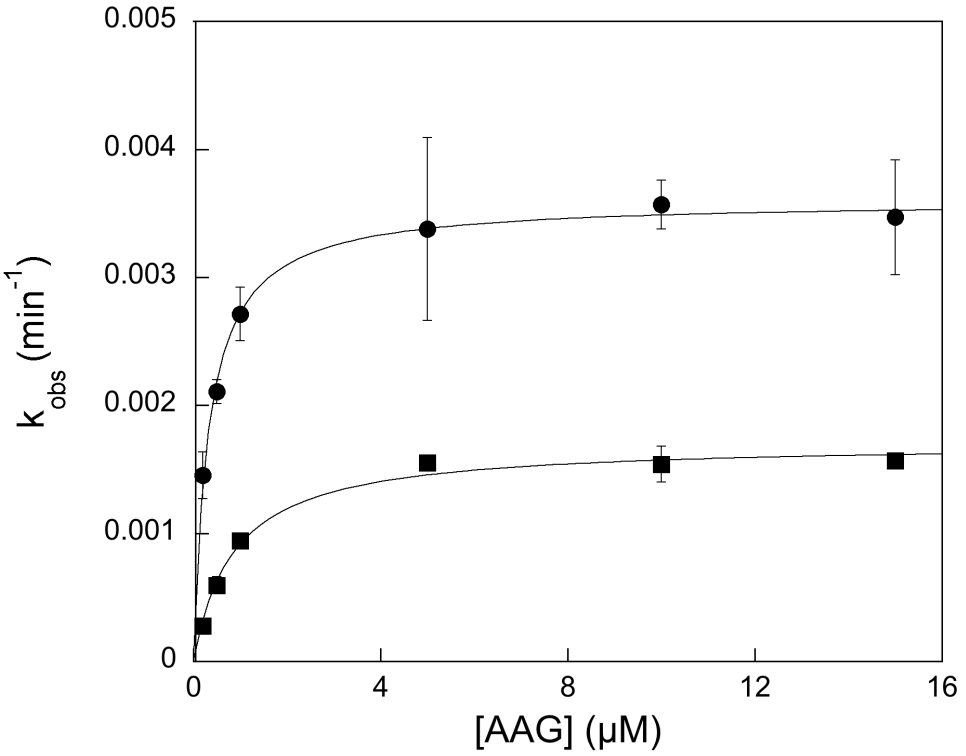

SUPPORTING REFERENCES

(1) O'Brien, P. J.; Ellenberger, T. *Biochemistry* **2003**, *42*, 12418-29.
(2) Baldwin, M. R.; O'Brien, P. J. *Biochemistry* **2009**, *48*, 6022-33.
(3) Hedglin, M.; O'Brien, P. J. *Biochemistry* **2008**, *47*, 11434-45.
(4) Watkins, N. E., Jr.; SantaLucia, J., Jr. *Nucleic Acids Res* **2005**, *33*, 6258-67.
(5) O'Brien, P. J.; Ellenberger, T. *J Biol Chem* **2004**, *279*, 9750-7.
(6) Saparbaev, M.; Mani, J. C.; Laval, J. *Nucleic Acids Res* **2000**, *28*, 1332-9.
(7) Wyatt, M. D.; Samson, L. D. *Carcinogenesis* **2000**, *21*, 901-8.
(8) Asaeda, A.; Ide, H.; Asagoshi, K.; Matsuyama, S.; Tano, K.; Murakami, A.; Takamori, Y.; Kubo, K. *Biochemistry* **2000**, *39*, 1959-65.
(9) Lau, A. Y.; Scharer, O. D.; Samson, L.; Verdine, G. L.; Ellenberger, T. *Cell* **1998**, *95*, 249-58.
(10) Lau, A. Y.; Wyatt, M. D.; Glassner, B. J.; Samson, L. D.; Ellenberger, T. *Proc Natl Acad Sci U S A* **2000**, *97*, 13573-8.
(11) Abner, C. W.; Lau, A. Y.; Ellenberger, T.; Bloom, L. B. *J Biol Chem* **2001**, *276*, 13379-87.
(12) Saparbaev, M.; Laval, J. *Proc Natl Acad Sci U S A* **1994**, *91*, 5873-7.
(13) Hitchcock, T. M.; Dong, L.; Connor, E. E.; Meira, L. B.; Samson, L. D.; Wyatt, M. D.; Cao, W. *J Biol Chem* **2004**, *279*, 38177-83.
(14) Lee, C. Y.; Delaney, J. C.; Kartalou, M.; Lingaraju, G. M.; Maor-Shoshani, A.; Essigmann, J. M.; Samson, L. D. *Biochemistry* **2009**, *48*, 1850-61.
(15) Cao, C.; Jiang, Y. L.; Krosky, D. J.; Stivers, J. T. *J Am Chem Soc* **2006**, *128*, 13034-5.
(16) Cao, C.; Jiang, Y. L.; Stivers, J. T.; Song, F. *Nat Struct Mol Biol* **2004**, *11*, 1230-6.
(17) Krosky, D. J.; Schwarz, F. P.; Stivers, J. T. *Biochemistry* **2004**, *43*, 4188-95.
(18) Krosky, D. J.; Song, F.; Stivers, J. T. *Biochemistry* **2005**, *44*, 5949-5959.